World J Surg (2019) 43:2595–2606
https://doi.org/10.1007/s00268-019-05055-2

ORIGINAL SCIENTIFIC REPORT WITH VIDEO

# The Application of Indocyanine Green Fluorescence Imaging During Robotic Liver Resection: A Case-Matched Study

**Marco Vito Marino[1,2] · Salomone Di Saverio[3] · Mauro Podda[4] · Marcos Gomez Ruiz[2] · Manuel Gomez Fleitas[5]**

Published online: 20 June 2019


## Abstract

*Background* The ICG fluorescence properties are progressively gaining momentum in the HPB surgery. However, the exact impact of ICG application on surgical outcomes is yet to be established.

*Methods* Twenty-five patients who underwent ICG fluorescence-guided robotic liver resection were case-matched in a 1:1 ratio to a cohort who underwent standard robotic liver resection.

*Results* In the ICG group, six additional lesions not diagnosed by preoperative workup and intraoperative ultrasound were identified and resected. Four of the lesions were proved to be malignant. Despite the similar operative time (288 vs. 272 min, $p = 0.778$), the risk of postoperative bile leakage (0% vs. 12%, $p = 0.023$), R1 resection (0% vs. 16%, $p = 0.019$) and readmission ($p = 0.023$) was reduced in the ICG group compared with the no-ICG group.

*Conclusions* The ICG fluorescence is a real-time navigation tool which enables surgeons to enhance visualization of anatomical structures and overcome the disadvantages of minimally invasive liver resection. The procedure is not time-consuming, and its applications can reduce the postoperative complication rate in robotic liver surgery.

**Electronic supplementary material** The online version of this article (https://doi.org/10.1007/s00268-019-05055-2) contains supplementary material, which is available to authorized users.

✉ Marco Vito Marino
marco.vito.marino@gmail.com

[1] Department of Emergency and General Surgery, Azienda Ospedaliera Ospedali Riuniti "Villa Sofia-Cervello", Via Trabucco 180, 90146 Palermo, Italy

[2] Department of Colorectal and General Surgery, Hospital Universitario Marqués de Valdecilla, Av. Valdecilla 25z, 39008 Santander, Spain

[3] Cambridge Colorectal Unit, Addenbrooke'S University Hospital NHS Foundation Trust, Hills Road, Cambridge CB2 0QQ, UK

[4] Department of General, Emergency and Minimally Invasive Surgery, Cagliari University Hospital "Policlinico D. Casula", SS 554 Km 4,500, 09142 Cagliari, Italy

[5] Departamento de Innovación Y Cirugía Robótica, Hospital Universitario Marqués de Valdecilla, Av. Valdecilla 25, 39008 Santander, Spain

## Introduction

Firstly used as a reagent for estimating hepatic function before liver surgery, the fluorescence properties of indocyanine green (ICG) were applied in hepatobiliary surgery since the late 2000s for the intraoperative identification of hepatobiliary structures [1, 2].

Its exclusive and selective hepatic metabolism and its bile excretion enable the visualization of the extrahepatic bile duct anatomy, and thus, it can help identify insufficiently closed bile duct stumps in the hepatic transection surface [3, 4].

Since ICG accumulates in cancerous tissues of hepatocellular carcinoma (HCC) and in noncancerous hepatic parenchyma around adenocarcinoma foci, its application was later extended to the identification of small subcapsular liver tumors prior to hepatic transection [5]. Since 2008, it was adopted in the dye-staining method for the identification of segmental boundaries of the liver, thus

overcoming the previous limitations encountered in patients with liver cirrhosis or with severe adhesions on the liver surface during the application of indigo carmine or Glissonean sheaths clamping [2, 6].

Lastly, it is used during living-donor liver transplantation to estimate the portal uptake function in veno-occlusive regions of the liver or to assess the patency of the reconstructed hepatic artery and portal vein and for intraoperative laparoscopic detection of extrahepatic metastasis in HCC patients, hepatic micrometastasis of pancreatic cancer and bile duct infiltration of intrahepatic cholangiocarcinomas [7–11].

Although some experience with ICG staining technique during laparoscopic anatomical resection was reported offering promising results, the direct or transhepatic injection of ICG solution into the portal vein for the staining method is technically challenging due to the impaired dexterity and limited access [12].

The robotic approach can potentially overcome these limitations thanks to the stability of the platform, magnified three-dimensional high-definition vision and increased degree of freedom of the instruments, which translates into an enhanced microdissection and microsuturing capabilities and higher dexterity.

These capabilities can be crucial in surgical interventions that require meticulous dissection, clear exposure and accurate bleeding control. Moreover, the software for indocyanine green fluorescence (ICG-F) (Firefly$^{TM}$) is integrated in the robotic system, thus enabling to perform a three-dimensional intraoperative cholangiography with real-time visualization of fluorescence imaging.

The potential advantages of the use of ICG fluorescence imaging in the setting of robotic liver resection over the laparoscopic and open approaches are related to the possibility to perform liver resections using the association of the 3D vision and the fluorescence imaging and the possibility to perform an intraoperative 3D cholangiography.

To the best of our knowledge, all the retrospective robotic large ( $>$ 20 cases) series so far have analyzed the ICG application exclusively during cholecystectomy [13]. Until now, no studies addressed the application of ICG during robotic liver resection.

After describing our initial experience in robotic liver surgery, we decided to investigate and analyze the effects of the application of ICG fluorescence imaging on the outcomes of patients who underwent robotic liver resection, performing a 1:1 case-matched comparison of 25 patients who underwent robotic liver surgery with or without the application of ICG [14, 15].

## Methods

### Patient Selection and Workup

From May 2014 to April 2018, 25 patients operated for malignant liver tumors by robotic approach with ICG staining were matched with patients for whom the ICG was not used, in a 1:1 ratio. Comparable by age, sex, body mass index (BMI), American Society of Anesthesiologists (ASA) score, tumor size and location, control group patients were selected to ensure similar baseline characteristics and to minimize the effect of potential selection bias.

The choice between ICG versus no-ICG method was dependent on the availability of the dye, as well as on patient's choice and iodine allergy.

The study was conducted after the approval of the Institutional Ethics Review Board and performed according to the Helsinki Declaration guidelines. A written informed consent was signed and obtained from all the patients after the explanation of the surgical procedure and the study purpose. All clinical cases were discussed at a preoperative multidisciplinary meeting conference, and all patients were considered eligible for robotic approach if no contraindication was present (Table 1).

The preoperative workup included whole-body contrast-enhanced computed tomography (CT), liver gadoxetic acid-enhanced magnetic resonance imaging (MRI), abdominal ultrasound, tumor markers and routine blood examination. Hepatitis screening was performed by measurement of hepatitis B surface antigen and hepatitis C antibody. Liver function was assessed with Child–Pugh score. An ICG skin test was performed before surgery, and the estimated residual liver function was based on the ICG (0.5 mg/Kg body weight) retention rate at 15 min after intravenous administration (ICGR15) generally five days before surgery.

### Definitions

Surgical procedures were classified according to the Brisbane terminology [16].

The complications were classified according to the Clavien-Dindo score [17]. The definition of post-hepatectomy liver failure (PHLF) was done according to the definition of ISGLS (International Study Group of Liver Surgery) [18]. Bile leakage was defined as bilirubin concentration in the drain fluid at least 3 times the serum bilirubin concentration on or after postoperative day 3 or as the need for radiologic or operative intervention resulting from biliary collections or bile peritonitis [19]. Intraoperative blood loss was quantified by measuring the fluid from

**Table 1** Exclusion criteria from the study

| |
|---|
| Lesions with extensive subcapsular involvement |
| Lesions invading major vessels (inferior vena cava or hepatic veins) |
| Lesions with extensions into the diaphragm |
| Lesions with distant involvement or metastasis |
| Patients requiring simultaneous surgical procedures |
| Positive ICG skin test* |
| Patients who required colorectal resection |

*ICG skin test: a gauze with indocyanine green is put on the skin of the patient to check for hypersensitivity

the suction. In case of malignant disease, resection margins were classified by a margin to tumor distance $\geq$ 1 mm (R0) or as margin to tumor distance $<$ 1 mm (R1). Readmission and perioperative mortality were considered as those occurring during the same hospital stay or within 90 days after discharge.

## Technical Description

All operations were performed employing the Da Vinci Robotic Surgical System model Si® (Intuitive Surgical, Sunnyvale, CA, USA). In the ICG group, the Firefly™ mode was activated.

The preoperative intravenous administration of ICG served as a fluorescence source for intraoperative identification of hepatic tumors. The liver surface was inspected once the pneumoperitoneum was established, and three types of fluorescence pattern (total, partial or rim fluorescence) were identified and collected according to the accumulation of ICG [5].

After liver mobilization, the target Glissonean pedicle was dissected, encircled and temporally clamped after confirmation of blood supply to the preserved adjacent segment using intraoperative ultrasonography (IOUS). Three techniques of staining already described were selected based on findings of preoperative imaging and intraoperative ultrasound [20, 21]:

1. *Negative staining technique* the ICG was injected intravenously in a systemic vein (2.5 mg), after temporary closure/clamping of the corresponding tumor-bearing portal branch or of the hepatic region parenchyma to be removed, which appeared as a defect of fluorescence (dark/ ischemic) region (Figs. 1, 2). The negative staining technique was used when the tumor-bearing portal vein (PV) was occluded because of tumor invasion or PV embolization;
2. *Positive staining technique* the segment to be removed was stained and visualized after portal injection of ICG (2.5 mg) in 10 ml of saline solution through the puncture into the correspondent segmental tumor-bearing portal branch of a 16-gauge needle held by robotic Needle Driver™ (Fig. 3). Single (single-staining) or double (multiple-staining) injections were performed if single or multiple tumor-bearing portal branches were identified. Both artery and portal veins were occluded, after the injection, by Bulldog clamp, thus avoiding the washout of the dye. The hepatic parenchyma to be removed appeared stained (green);
3. *Counterstaining technique* in this case the ICG injection was performed on the portal branch bearing hepatic parenchyma which should be preserved. It was adopted when the tumor-bearing PV had already been invaded by tumor tissue or tumoral thrombus and its clamping/closure was not feasible. The hepatic parenchyma to remove appeared not stained.

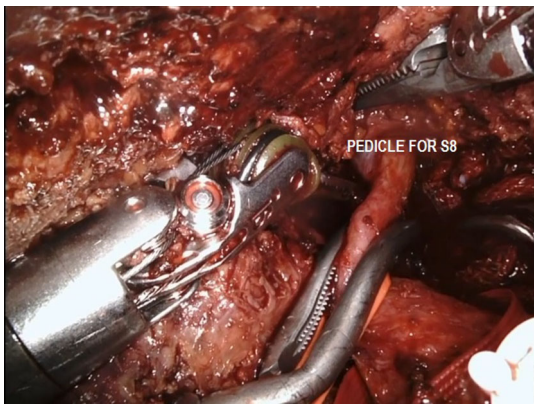


**Fig. 1** Clamping of the segment 8 (s8) portal pedicle, during a negative staining technique

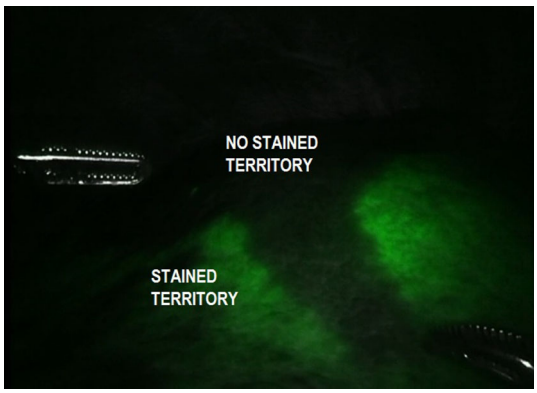


**Fig. 2** Visualization of the stained territory on the liver surface

In all cases, once the ICG-stained area appeared, the parenchymal transection was initiated along the interface between the green and the dark areas using the Pringle maneuver. A transection line was marked with Da Vinci

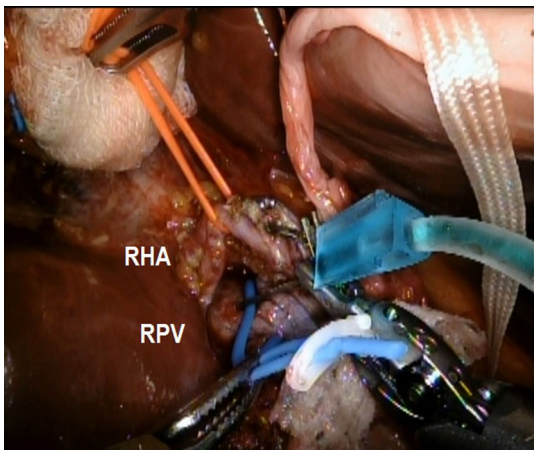


**Fig. 3** The ICG solution is injected into the right portal vein (RPV). The right hepatic artery (RHA) is dissected and exposed


**Fig. 4** The transection line along the stained/no-stained area is marked with robotic Monopolar Scissor™

Monopolar Scissors™ following the discoloration line on liver surface (Fig. 4).

In all cases the Firefly™ mode was activated from the robotic console during the parenchymal transection to determine the hepatic transection line, the biliary confluence and the surgical margins.

After the specimen removal and once the hepatic transection was completed, a cholangiography catheter was inserted into the cystic duct and secured (Fig. 5). A diluted ICG solution was injected into the bile duct, while the common bile duct was temporarily occluded by Bulldog clamp distal to the cystic duct insertion.

Next, the Firefly™ mode was again activated, while a gentle irrigation of the liver surface was performed to visualize possible biliary leaks from the hepatic remnant. In case of bile leakage, the sites were robotically closed by suture of 4–0 Prolene®.

The sections of the surgical specimen were postoperatively observed for their near-infrared fluorescence (NIF) using a charge-coupled device (CCD) camera and a xenon light photodynamic emission (PDE) camera (Hamamatsu Photonics, Hamamatsu).

### Statistical Analysis

Continuous data are expressed as medians (range), and categorical variables as numbers (percentage). Categorical and continuous data were compared using Fisher's exact test and the Wilcoxon rank-sum test, respectively. Statistical analysis was performed using SPSS 12 (SPSS Inc., Chicago, IL). A p value $< 0.05$ was considered to indicate statistical significance.

## Results

A total of 50 patients, 25 for each cohort (ICG and no-ICG), underwent robotic liver resection from May 2014 to April 2018, and they were enrolled in this study. Their average age was 66.2 years (range, 35–78) in the ICG group and 64.6 years (range, 33–77) in the no-ICG group.

The two cohorts were well matched for age, gender, BMI, tumor number and size, and pathological examination (Table 2). Two patients underwent preoperative portal vein embolization.

In both groups, the main indication for surgery was colorectal liver metastasis (CRLM), with 31 cases. Among the 25 patients belonging to each cohort, 11 underwent major hepatectomy.

Six Pringle maneuvers were performed in each group.

Overall, 28 and 27 lesions were detected preoperatively in ICG and no-ICG groups, respectively.

The operating time (288 vs. 272 min, $p = 0.778$), blood loss (270 vs. 255 ml, $p = 0.675$) and the length of hospital stay (7.2 vs. 7.4 days, $p = 0.922$) did not differ significantly between the two groups (Table 3).

### Bile Leak

In the ICG group, we observed a lower bile leakage (0% vs. 12%, $p = 0.023$) and post-hepatectomy liver failure (PHLF) rate (4% vs. 12%, $p = 0.035$) in comparison with no-ICG group.

Overall, three patients in the no-ICG group were readmitted, one for bile leakage grade B and two for abscess formation. Both required percutaneous CT-guided drainage. The overall morbidity rate was slightly higher in the no-ICG group (36% vs. 20%, $p = 0.343$), although not statistically significant (Table 4).

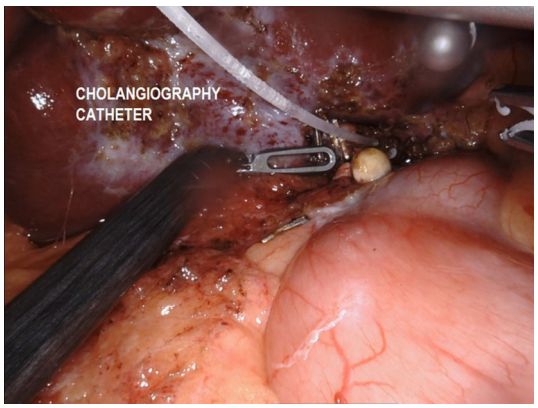


**Fig. 5** Insertion of the cholangiography catheter into the cystic duct during a liver segmentectomy

**Table 2** Demographic and preoperative characteristics of the two cohorts of patients (ICG vs no-ICG)

| | ICG | No-ICG | *p* value |
|---|---|---|---|
| No. of patients | 25 | 25 | \ |
| Age, years (range) | 66.2 (35–78) | 64.6 (33–77) | 0.634 |
| Sex (male/female), ratio | 14:11 | 13:12 | 0.822 |
| BMI, Kg/m$^2$ (range) | 23.2 (17.5–27) | 22.9 (18.1–27.6) | 0.886 |
| ASA I/II/III score | 7/14/4 | 5/15/5 | 0.628 |
| ICG-R15, % (range) | 15.4% (7.2–24) | 14.6% (8.4–28.5) | 0.437 |
| Child–Pugh score A, n | 20 | 20 | 1 |
| Child–Pugh score B, n | 5 | 5 | 1 |
| Hepatitis B, n | 3 | 2 | 0.776 |
| Hepatitis C, n | 1 | 2 | 0.625 |
| Liver cirrhosis, n | 3 | 2 | 0.788 |
| Tumor diameter, mm (range) | 23.5 (2–47) | 23.9 (5–52) | 0.717 |
| Number of tumors, n | 28 | 27 | 0.887 |
| Indication, n | | | 0.744 |
| HCC | 7 | 9 | 0.437 |
| Well differentiated | 4 | 6 | |
| Moderately differentiated | 2 | 2 | |
| Poorly differentiated | 1 | 1 | |
| CRLM | 16 | 15 | 0.823 |
| ICC | 2 | 1 | 0.845 |
| Previous surgery, n | 4 | 3 | 0.567 |

*BMI* body mass index, *ASA* American Society of Anesthesiologists, *ICG-R15* indocyanine green retention rate at 15 min, *HCC* hepatocellular carcinoma, *CRLM* colorectal liver metastasis, *ICC* intrahepatic cholangiocellular carcinoma

## Resection Margins Analysis

All the tumors detected by the ICG were completely removed. The mean resection margin was slightly lower in the ICG group compared to no-ICG (13 vs. 22 mm, $p = 0.088$). A reduced R1 resection rate was reported in the ICG group compared to no-ICG (0 vs. 4, $p = 0.019$).

## Oncological Outcomes

Despite all four patients with newly malignant ICG-detected microtumors treated by complete metastases resection, all of them developed hepatic relapse at 1-year follow-up.

All of these patients presented with multiple CRLMs involving the right liver lobe, and two of them were treated with radiofrequency ablation. Two patients are currently scheduled for redo liver resections.

Two patients died at 1-year. Myocardial infarction was the cause of death in one patient, whereas pulmonary embolism occurred in one patient with systemic spread of cancer disease.

The 1- and 2-year overall survival rates were 92% and 89%, respectively, in the ICG group and 91.5% and 87% in the no-ICG group. The 1- and 2-year disease-free survival rates were 76% and 77%, respectively, in the ICG group and 72.5% and 69% in the no-ICG.

## Tumor Detection

The fluorescence targeted 34 lesions in the ICG group. It detected six lesions more than that revealed by the preoperative imaging examination and intraoperative ultrasound. We observed the following tumoral patterns: 8 total-type fluorescence, 6 partial-type fluorescence and 20 rim-like fluorescence pattern, with a selective accumulation of ICG fluorescence at the marginal region of the tumor (Table 5).

The newly detected ICG lesion was as small as 3 mm in size (range 3–9 mm), all located within 7 mm from liver surface. Four out of the six lesions not identifiable at white-light color imaging were malignant at the final pathology. Two rim pattern tumors were in fact a steatosis area and an hemangioma, thus confirming the high risk of false positive lesion. In both cases the patients had impaired liver function, in which the ICG removal from noncancerous tissue was insufficient.

While the ICG fluorescence of liver surface detected overall six tumors more than intraoperative ultrasonography (34 vs. 28), it failed to detect three tumors confirmed by the fluorescence imaging of the resected specimens.

All missed tumors had similar mean diameter (3.5 vs. 3.3 mm) compared to the identifiable tumors but were located deeper (more than 8 mm from liver surface) into

**Table 3** Surgical outcomes of the two cohorts of patients (ICG vs. NO-ICG)

| | ICG ($n$ = 25) | No-ICG ($n$ = 25) | $p$ value |
|---|---|---|---|
| Type of resection, *n* | | | 0.566 |
| Right hepatectomy | 8 | 7 | |
| Left hepatectomy | 3 | 4 | |
| Segmentectomy | 12 | 11 | |
| Bisegmentectomy | 2 | 3 | |
| Operation time, min (range) | 288 (155–538) | 272 (123–652) | 0.778 |
| Estimated blood loss, ml (range) | 270 (65–945) | 255 (50–885) | 0.675 |
| Blood transfusion, *n* | 1 | \ | 0.448 |
| Inflow occlusion, min (range) | 35 (31–74) | 46 (29–66) | 0.332 |
| Length of hospital stay, days (range) | 7.2 (5–11) | 7.4 (5–16) | 0.922 |
| conversion, *n* | \ | \ | |
| Bile leakage, *n* (%) | \ | 3 (12%) | *0.023* |
| PHLF, *n* (%) | 1 (4%) | 3 (12%) | *0.035* |
| Liver abscess, *n* | \ | 2 | 0.179 |
| Resection margin, mm (range) | 13 (5–22) | 22 (0–52) | 0.088 |
| R1 | 0 | 4 | *0.019* |
| R0 | 25 | 21 | 0.216 |
| Readmission, *n* | \ | 3 | 0.023 |
| Reoperation, *n* | \ | 1 | 0.567 |
| Pattern of recurrence, *n* | 5 | 4 | 0.786 |
| Intrahepatic recurrence | 4 | 3 | 0.883 |
| Extrahepatic recurrence | \ | 1 | 0.646 |
| Mortality, *n* | \ | 1 | 0.567 |

*PHLF* post-hepatectomy liver failure. *In Italic $p$ value $< 0.05$

**Table 4** Classification of the complications occurred in the two cohorts of patients (ICG vs NO-ICG)

| | ICG ($n$ = 25) | No-ICG ($n$ = 25) | $p$ value |
|---|---|---|---|
| Overall morbidity, n (%) | 5 (20%) | 9 (36%) | 0.343 |
| *Minor (Clavien I – II)* | | | |
| Bile leakage (grade A) | \ | 2 | 0.179 |
| Fluid collection | 1 | \ | 0.678 |
| PHLF (grade A) | 1 | 1 | 1 |
| Liver abscess | \ | 2 | 0.179 |
| Wound infection | 1 | \ | 0.668 |
| Pleural effusion | 1 | \ | 0.668 |
| *Major (Clavien III–V)* | | | |
| Bile leakage (grade B) | \ | 1 | 0.678 |
| Postoperative bleeding | 1 | \ | 0.678 |
| PHLF (grade B) | \ | 2 | 0.179 |
| Pulmonary embolism | \ | 1 | 0.697 |

*PHLF* post-hepatectomy liver failure

the liver parenchyma. The pathological examination confirmed to be one intrahepatic cholangiocarcinoma and two poorly differentiated HCCs, and they resulted in a partial fluorescence pattern at the fluorescence examination of the resected specimens.

The ICG fluorescence imaging clearly identified all of the microscopically confirmed malignant tumors 'ex vivo' on the cut surface of the resected specimens showing a tumor detectability of 100%.

### Fluorescence Pattern

Comparing the pattern of fluorescence of the liver surface and that of sectioned surgical specimens, we observed a discrepancy only in four cases, resulting in rim fluorescence instead of partial fluorescence imaging pattern. Overall, the ICG fluorescence of sectioned specimens revealed 8 fluorescence-type, 5 partial and 24 rim-type fluorescence lesions. The final pathological examination confirmed that all 8 cases of total fluorescence-type tumors were well-differentiated HCC, but only 18 cases of the 24 rim-type consisted of CRLM, while 6 patients had lesions classified as moderately or poorly differentiated HCC.

### Staining Technique

The staining techniques applied for visualization of the hepatic boundaries were classified as follows: 13 negative, 8 positive and 4 counterstaining methods.

The negative technique was used for six major hepatectomies and seven segmentectomies. Conversely, the positive staining method was used for three major hepatectomies and five segmentectomies, two of whom underwent preoperative portal vein embolization.

Two right hepatectomies and two bisegmentectomies were performed with the counterstaining technique. Details on types of liver resection performed, tumor localization, tumor histology and staining technique are shown in Table 6.

The median duration between ICG administration and portal vein territory visualization was higher for the negative staining technique (390 s), whereas the most rapid was the positive staining technique (110 s). The counterstaining technique, applied four times, had an overall visualization time of 220 s.

For the positive staining technique, several puncture numbers were required in two patients for malposition of the needle. In three patients with chemotherapy-induced steatohepatitis, we had an unclear visualization of the portal vein territory.

The negative method offered uniform and reproducible staining of the liver also in patients who underwent previous liver resection or chemotherapy administration. In four out of eight patients (50%), the positive staining method produced unclear fluorescence pattern.

Three biliary leakages (12%) were identified at the liver resection surface employing the fluorescence mode. They were sutured, and no patient in the ICG group experimented bile leakage.

## Discussion

The ICG-based fluorescence-guided surgery relies on the fluorescence signal, peaking at about 840 nm, emitted by plasma protein-bound ICG (fluorophore) after being illuminated by a specific near-infrared light source (750–810 nm). It is an intraoperative navigation tool, which allows the enhanced visualization of anatomical structures through connective tissue 5–10 mm thick, and it helps to guide the surgical procedures and provide the surgeon with enhanced visualization of anatomical structures and real-time understanding of an organ perfusion [22] .

The ICG-based fluorescence imaging has been already applied in oncologic surgery to delineate the lymphatic system or to detect sentinel lymph nodes in patients with esophageal, gastric, breast, colorectal and skin cancer [23–27].

**Table 5** Tumor detectability and fluorescence pattern classification after the application of indocyanine green fluorescence (ICG-F)

| | ICG-F of the liver surface | ICG-F of the resected specimens |
|---|---|---|
| Total number of tumors detected, *n* | 34 | 37 |
| Total-type, *n* | 8 | 8 |
| Partial-type, *n* | 6 | 5 |
| Rim-type, *n* | 20 | 24 |
| Size, mm (range) | 3.5 (3–8) | 3.3 (3–7) |
| Sensitivity of tumor detectability (%) | 85% | 100% |

**Table 6** Case analysis of type of liver resection, tumor localization, staining technique and tumor histology

| Patient *N* | Type of liver resection | Tumor localization | Staining technique | Tumor histology |
|---|---|---|---|---|
| 1 | Right hepatectomy | S5 + S6 | Negative | CRLM |
| 2 | Segmentectomy | S7 | Negative | ICC |
| 3 | Right hepatectomy | S7 + S6 + S5 | Positive | CRLM |
| 4 | Segmentectomy | S2 | Negative | HCC |
| 5 | Right hepatectomy | S8 + S5 + S6 | Negative | CRLM |
| 6 | Right hepatectomy | S8 + S6 + S5 | Counterstaining | CRLM |
| 7 | Left hepatectomy | S4 + S3 | Negative | CRLM |
| 8 | Segmentectomy | S3 | Positive | HCC |
| 9 | Right hepatectomy | S5 + S6 | Negative | CRLM |
| 10 | Bisegmentectomy | S5 + S8 | Counterstaining | CRLM |
| 11 | Segmentectomy | S5 | Positive | ICC |
| 12 | Right hepatectomy | S6 + S7 + S5 | Counterstaining | CRLM |
| 13 | Segmentectomy | S7 | Negative | HCC |
| 14 | Segmentectomy | S4 | Negative | HCC |
| 15 | Right hepatectomy | S5 + S8 + S6 | Positive | CRLM |
| 16 | Segmentectomy | S8 | Negative | HCC |
| 17 | Left hepatectomy | S4 + S2 | Negative | CRLM |
| 18 | Segmentectomy | S4 | Positive | HCC |
| 19 | Right hepatectomy | S7 + S5 + S6 | Negative | CRLM |
| 20 | Bisegmentectomy | S6 + S7 | Counterstaining | CRLM |
| 21 | Segmentectomy | S8 | Negative | CRLM |
| 22 | Left hepatectomy | S3 + S4 | Positive | CRLM |
| 23 | Segmentectomy | S4 | Negative | HCC |
| 24 | Segmentectomy | S5 | Positive | CRLM |
| 25 | Segmentectomy | S6 | Positive | CRLM |

*CRLM* colorectal liver metastases, *ICC* intrahepatic cholangiocellular carcinoma, *HCC* hepatocellular carcinoma

Furthermore, the assessment of real-time visceral perfusion has been adopted for the identification of the optimal resection site and estimation of the blood supply of the visceral anastomosis in both colorectal and upper gastrointestinal surgeries with the potentiality to eliminate dehiscence due to inadequate vascularization [28–30]. Recently, it was also applied to mark endoscopically the tumor site and to detect early foci of peritoneal carcinomatosis [31, 32].

As laparoscopic and robotic fluorescence systems were developed for clinical settings, ICG fluorescence imaging was rapidly extended to minimally invasive abdominal surgery.

Recognition of vascular and biliary anatomy is important in hepatic surgery and could help to decrease intraoperative complications, especially in the presence of anatomical variations and in case of surgeons within their learning curve [33].

Since 2010, the software for the near-infrared fluorescence imaging system was integrated into the surgeon console of the Da Vinci Si HD platform, thus displaying the information in real time without switching the sight between the operative field and the monitor so it without interfering with the surgical workflow. Robotic technology offers a dynamic technological interface where several sources of information and many potential innovations like near-infrared fluorescence, 3D ultrasound instruments and augmented reality software can be easily implemented.

In this scenario, the possibility to combine the advantages of a high-definition 3D vision, associated with a real-time enhancement of keys anatomical structures, highlights all the advantages of the ICG technique.

In our experience, the intraoperative fluorescence imaging following preoperative injection of ICG detected all 37 microscopically malignant tumors on the cut surface of the resected specimens, confirming the high tumor detectabilities reported by Nakaseko et al. [34].

Furthermore, the intraoperative exploration of liver surface through ICG fluorescence identified six small

subcapsular hepatic tumors not detected in the preoperative imaging in our series.

This can be helpful not only during laparoscopic hepatectomy in which the tactile feedback is compromised [35], but also in open surgery in case of cirrhosis or for patients who have undergone multiple chemotherapy cycles and so the liver parenchyma is hardened and intraoperative ultrasound is challenging [36, 37].

Because ICG labeling is not specific, benign lesions may also emit fluorescence. In our experience, two out of the six new lesions were benign at final pathology, and both of them were detected in cirrhotic patients. In case of impaired liver function, liver cirrhosis or in the presence of liver regeneration nodules, the ICG removal/excretion from noncancerous tissue can be insufficient or delayed, thus increasing the rate of false positive results.

The high sensitivity reported for identification of liver tumors with the use of intraoperative fluorescence imaging on liver surface is quite promising, but actually there are no widely accepted guidelines that report the defined doses and the timing for the intraoperative use of ICG-based fluorescence [35, 38, 39]. Furthermore, the low depth penetration (up to 8 mm from the hepatic surface) still requires the need for intraoperative ultrasonography [40].

The application of ICG fluorescence could help to ensure complete tumor resection and adequate free tumor margin resection, as a clear boundary between tumor ring of metastatic lesion and normal tissues or as the absence of residual fluorescence at the end of surgical procedure [41]. It is particularly ideal for tiny ( $< 5$ mm) liver metastasis and superficial liver tumors as well as in neoplasm with bile duct infiltration [9, 42].

The fluorescence imaging system associated with robotics offers additional information to the surgeon regarding anatomy, blood perfusion, lymphatic drainage and functional liver reserve.

Our data confirmed these potentialities in terms of reduced R1 resection rate (0 vs. 4, $p = 0.019$), despite the surgical margin being smaller in the ICG group compared to no-ICG group (13 vs. 22 mm, $p = 0.088$). According to our initial results, the ICG can lead potentially to a tailored-surgery approach, thus favoring parenchymal sparing liver resections.

Three types of fluorescence pattern (uniform fluorescence, partial or rim fluorescence) were identified according to the experience by Ishizawa et al. on ICG accumulation in liver tumors [5].

These patterns are theoretically associated with the pathological characteristics and differentiation of liver tumors: Total heterogeneous fluorescence-type included all well-differentiated HCC, whereas rim fluorescence-type consisted of a fluorescence corona-like pattern typical of poorly differentiated HCC and CRLM. In our experience, we registered only a slight discrepancy between the ICG fluorescence visualization of the liver surface in comparison to that of resected liver specimens, resulting in a lesion with rim fluorescence pattern instead of a partial fluorescence. Furthermore, despite all total fluorescence-type lesions confirmed to be well-differentiated HCC at the final pathological diagnosis, both partial-type and rim-type fluorescence patterns resulted to be CRLM or poor/moderately differentiated HCC; thus, if the former confirmed to be a potential diagnostic tool for HCC, the latter provides a unpredictable final diagnosis.

As showed by Aoki et al., the detection rate of liver segments boundaries after ICG staining technique is high (90%), and it allows accurate visualization even in the case of liver cirrhosis [43]. Furthermore, it offered better results compared to indigo carmine in terms of accuracy of anatomical segmentectomy (100% vs. 57%), especially in patients who underwent repeated liver resection for recurrence [44].

The recent adoption of ICG offers promising results, and several ways of ICG administration (single- or multiple-staining, counterstaining, negative staining or paradoxical negative staining technique) were described. The safety of this approach in terms of low morbidity was already demonstrated in other laparoscopic series, and it can be a valuable tool in case of aberrant anatomy, thus avoiding leaving behind areas of ischemic of liver parenchyma, which may result in abscess formation [45].

In our experience, the negative staining technique was found simpler and more feasible, as confirmed by the fact that it was generally employed for lesions located in the superior segments.

The direct ICG injection into a portal vein branch is particularly challenging and stressful, as it requires a wide dissection of the portal vein to be injected, a gentle traction on it and finally a careful manipulation of the needle by fine robotic instruments. Within this context, we can confirm that the endowristed instrumentation of the robotic system makes the positive staining technique easier to perform.

Generally after the ICG injection through portal vein, fluorescence developed rapidly within 2–3 min (overall time, 110 s). With an ICG injection in the systemic vein, fluorescence developed later on in 5–10 min (overall time, 390 s). A Pringle maneuver was necessary for reducing the washout of the dye and perpetual visualization of the segment.

Although biliary excretion of ICG can be detected shortly after the intravenous injection, the background contrast signal of liver parenchyma makes it less evident. Theoretically, it should be administered at least 15 min before imaging, but its maximum concentration is reached within 2 h.

In our experience, the fluorescence cholangiography was crucial to confirm the confluence between the right and left hepatic ducts on the hepatic hilum reducing the risks of bile duct injury or stenosis during major liver resections. Its use as a real-time tool for the detection of bile leaks on the hepatic transection surface or stumps of the hepatic ducts after the removal of specimen helped us to prevent post-operative biliary fistula in the ICG group, confirming the results of the controlled trial by Kaibori et al. [46]. The intraoperative cholangiography was not time-consuming in our experience. Moreover, it did not require the use of fluoroscopic C-arm that generally slows down the surgical workflow and expose the surgical team to ionizing radiations.

Despite the study having some limitations, such as its single-institutional setting, small sample size, short follow-up period and the heterogeneity of liver tumors included which could preclude robust conclusions regarding the resection margin width and oncologic outcomes, to the best of our knowledge this is the first fully robotic case-matched series which investigate the application of ICG in liver surgery.

Up to now, only one case series reported an initial experience in ICG fluorescence application during robotic liver surgery, but it includes both laparoscopic and robotic surgeries [47].

The aim of the future studies will be to investigate the correct administration time and enable the software to quantify the grade of fluorescence intensity. New cancer-specific fluorophores conjugated to monoclonal antibodies may provide a better specificity for detecting surface-invisible malignant liver tumor, as reported with the initial application of 5-aminolevulinic acid [48].

A novel specific fluorescence probe (γ-glutamyl hydroxymethyl rhodamine green gGlu-HMRG) is also progressively used for the visualization of adenocarcinoma foci in the specimens [49]. They enable a real-time in vivo microscopy for evaluation of resection margins, as well as accurate identification of metastatic versus normal lymph nodes or extrahepatic metastases of HCC [50, 51].

In conclusion, the ICG fluorescence enables surgeons to enhance visualization of anatomical structures and overcome the disadvantages of minimally invasive liver resection. While the surgeon can continue the surgical procedures without shifting his/her sight from the surgical field, the robot complements the use of ICG, thanks to its microdissection capabilities. The procedure is not time-consuming, and its applications can reduce the postoperative complication rate in robotic liver surgery.

**Author's Contribution** *MVM* contributed to study conception and design, acquisition, interpretation and analysis of data; drafting and critically revising the article for important intellectual content; and final approval of the version to be published. *SDS* was involved in interpretation and analysis of data; drafting and critically revising the article for important intellectual content; editing and revising the English for the final version to be published; and final approval of the version to be published. *MP* and *MGR* contributed to interpretation and analysis of data; drafting and critically revising the article for important intellectual content; and final approval of the version to be published. *MGF* was involved in study conception and design; interpretation and analysis of data; drafting and critically revising the article for important intellectual content; and final approval of the version to be published.

**Compliance with ethical standards**

**Conflict of interest** Marco Vito Marino, Salomone Di Saverio, Mauro Podda and Manuel Gomez Fleitas have no conflict of interest to disclose. Marcos Gomez Ruiz is Proctor and Advisor of Intuitive Surgical Inc., Medtronic, and Johnson & Johnson.

**Ethical approval** All procedures were in accordance with the ethical standards of the institutional and/or national research committee and with the 1964 Helsinki Declaration and its later amendments or comparable ethical standards. The study was conducted after the approval of the Institutional Ethics Review Board of Hospital Universitario Marquès de Valdecilla.

**Informed consent** Informed consent was obtained from all individual participants included in the study.

## References

1. Imamura H, Sano K, Sugawara Y et al (2005) Assessment of hepatic reserve for indication of hepatic resection: decision tree incorporating indocyanine green test. J Hepatobiliary Pancreat Surg 12:16–22
2. Aoki T, Yasuda D, Shimizu Y et al (2008) Image-guided liver mapping using fluorescence navigation system with indocyanine green for anatomical hepatic resection. World J Surg 32:1763–1767
3. Ishizawa T, Bandai Y, Kokudo N (2009) Fluorescent cholangiography using indocyanine green for laparoscopic cholecystectomy: an initial experience. Arch Surg 144:381–382
4. Mitsuhashi N, Kimura F, Shimizu H et al (2008) Usefulness of intraoperative fluorescence imaging to evaluate local anatomy in hepatobiliary surgery. J Hepatobiliary Pancreat Surg 15:508–514
5. Ishizawa T, Fukushima N, Shibahara J, et al (2009) Real-time identification of liver cancers by using indocyanine green fluorescent imaging. Cancer 115:2491–2504
6. Takasaki K (1998) Glissonean pedicle transection method for hepatic resection: a new concept of liver segmentation. J Hepatobiliary Pancreat Surg 5:286–291
7. Kawaguchi Y, Ishizawa T, Miyata Y et al (2013) Portal uptake function in veno-occlusive regions evaluated by real-time fluorescent imaging using indocyanine green. J Hepatol 58:247–253
8. Kubota K, Kita J, Shimoda M et al (2006) Intraoperative assessment of reconstructed vessels in living-donor liver transplantation, using a novel fluorescence imaging technique. J Hepatobiliary Pancreat Surg 13:100–104
9. Harada N, Ishizawa T, Muraoka A et al (2010) Fluorescence navigation hepatectomy by visualization of localized cholestasis from bile duct tumor infiltration. J Am Coll Surg 210:e2–6

10. Nanashima A, Tominaga T, Sumida Y et al (2018) Indocyanine green identification for tumor infiltration or metastasis originating from hepatocellular carcinoma. Int J Surg Case Rep 46:56–61
11. Yokoyama N, Otani T, Hashidate H et al (2012) Real-time detection of hepatic micrometastases from pancreatic cancer by intraoperative fluorescence imaging: preliminary results of a prospective study. Cancer 118:2813–2819
12. Ishizawa T, Zuker NB, Kokudo N et al (2012) Positive and negative staining of hepatic segments by use of fluorescent imaging techniques during laparoscopic hepatectomy. Arch Surg 147:393–394
13. Spinoglio G, Priora F, Bianchi PP et al (2013) Real-time near-infrared (NIR) fluorescent cholangiography in single-site robotic cholecystectomy (SSRC): a single-institutional prospective study. Surg Endosc 27:2156–2162
14. Marino MV, Shabat G, Guarrasi D, et al (2018) Comparative study of the initial experience in performing robotic and laparoscopic right hepatectomy with technical description of the robotic technique. Dig Surg doi: 10.1159/000487686
15. Marino MV, Gulotta G, Komorowski AL (2018) Fully robotic left hepatectomy for malignant tumor: technique and initial results. Updates Surg doi:10.1007/s13304-018-0560-2
16. Pang YY (2000) The Brisbane 2000 terminology of liver anatomy and resections. HPB 2:333–339
17. Clavien PA, Barkun J, de Oliveira ML, et al (2009) The Clavien-Dindo classification of surgical complications: five-year experience. Ann Surg 250:187–196
18. Sultana A, Brooke-Smith M, Ullah S, et al (2018) Prospective evaluation of the International Study Group for Liver Surgery definition of post hepatectomy liver failure after liver resection: an international multicentre study. HPB (Oxford) 20:462–469.
19. Koch M, Garden OJ, Padbury R et al (2011) Bile leakage after hepatobiliary and pancreatic surgery: a definition and grading of severity by the International Study Group of Liver Surgery. Surgery 149:680–688
20. Inoue Y, Arita J, Sakamoto T et al (2015) Anatomical liver resections guided by 3-dimensional parenchymal staining using fusion indocyanine green fluorescence imaging. Ann Surg 262:105–111
21. Kobayashi Y, Kawaguchi Y, Kobayashi K et al (2017) Portal vein territory identification using indocyanine green fluorescence imaging: Technical details and short-term outcomes. J Surg Oncol 116:921–931
22. Diana M (2017) Enabling precision digestive surgery with fluorescence imaging. Transl Gastroenterol Hepatol. 2017(2):97
23. Parungo CP, Ohnishi S, Kim SW et al (2005) Intraoperative identification of esophageal sentinel lymph nodes with near-infrared fluorescence imaging. J Thorac Cardiovasc Surg 129:844–850
24. Miyashiro I, Miyoshi N, Hiratsuka M et al (2008) Detection of sentinel node in gastric cancer surgery by indocyanine green fluorescence imaging: comparison with infrared imaging. Ann Surg Oncol 15:1640–1643
25. Kusano M, Tajima Y, Yamazaki K et al (2008) Sentinel node mapping guided by indocyanine green fluorescence imaging: a new method for sentinel node navigation surgery in gastrointestinal cancer. Dig Surg 25:103–108
26. Cahill RA, Anderson M, Wang LM et al (2012) Near-infrared (NIR) laparoscopy for intraoperative lymphatic road-mapping and sentinel node identification during definitive surgical resection of early-stage colorectal neoplasia. Surg Endosc 26:197–204
27. Tsujino Y, Mizumoto K, Matsuzaka Y et al (2009) Fluorescence navigation with indocyanine green for detecting sentinel nodes in extramammary Paget's disease and squamous cell carcinoma. J Dermatol 36:90–94
28. M HellanG Spinoglio A Pigazzi et al (2014) The influence of fluorescence imaging on the location of bowel transection during robotic left-sided colorectal surgery. Surg Endosc 28:1695–1702
29. Kumagai Y, Ishiguro T, Haga N et al (2014) Hemodynamics of the reconstructed gastric tube during esophagectomy: assessment of outcomes with indocyanine green fluorescence. World J Surg 38:138–143
30. Boni L, Fingerhut A, Marzorati A et al (2017) Indocyanine green fluorescence angiography during laparoscopic low anterior resection: results of a case-matched study. Surg Endosc 31:1836–1840
31. Watanabe M, Murakami M, Ozawa Y et al (2017) Intraoperative identification of colonic tumor sites using a near-infrared fluorescence endoscopic imaging system and indocyanine green. Dig Surg 34:495–501
32. Lieto E, Auricchio A, Cardella F et al (2018) Fluorescence-guided surgery in the combined treatment of peritoneal carcinomatosis from colorectal cancer: preliminary results and considerations. World J Surg 42:1154–1160
33. Giulianotti PC, Bianco FM, Daskalaki D et al (2016) Robotic liver surgery: technical aspects and review of the literature. Hepatobiliary Surg Nutr 5:311–321
34. Nakaseko Y, Ishizawa T, Saiura A (2018) Fluorescence-guided surgery for liver tumors. J Surg Oncol 118:324–331
35. Kudo H, Ishizawa T, Tani K et al (2014) Visualization of subcapsular hepatic malignancy by indocyanine-green fluorescence imaging during laparoscopic hepatectomy. Surg Endosc 28:2504–2508
36. Terasawa M, Ishizawa T, Mise Y et al (2017) Applications of fusion-fluorescence imaging using indocyanine green in laparoscopic hepatectomy. Surg Endosc 31:5111–5118
37. Gotoh K, Yamada T, Ishikawa O et al (2009) A novel image-guided surgery of hepatocellular carcinoma by indocyanine green fluorescence imaging navigation. J Surg Oncol 100:75–79
38. Tummers QR, Verbeek FP, Prevoo HA et al (2015) First experience on laparoscopic near-infrared fluorescence imaging of hepatic uveal melanoma metastases using indocyanine green. Surg Innov 22:20–25
39. Kawaguchi Y, Nagai M, Nomura Y et al (2015) Usefulness of indocyanine green-fluorescence imaging during laparoscopic hepatectomy to visualize subcapsular hard-to-identify hepatic malignancy. J Surg Oncol 112:514–516
40. Majlesara A, Golriz M, Hafezi M et al (2017) Indocyanine green fluorescence imaging in hepatobiliary surgery. Photodiagnosis Photodyn Ther 17:208–215
41. Zhang YM, Shi R, Hou JC et al (2017) Liver tumor boundaries identified intraoperatively using real-time indocyanine green fluorescence imaging. J Cancer Res Clin Oncol 143:51–58
42. van der Vorst JR, Hutteman M, Mieog JS et al (2012) Near-infrared fluorescence imaging of liver metastases in rats using indocyanine green. J Surg Res 174:266–271
43. Aoki T, Murakami M, Yasuda D et al (2010) Intraoperative fluorescent imaging using indocyanine green for liver mapping and cholangiography. J Hepatobiliary Pancreat Sci 17:590–594
44. Miyata A, Ishizawa T, Tani K et al (2015) Reappraisal of a dye-staining technique for anatomic hepatectomy by the concomitant use of indocyanine green fluorescence imaging. J Am Coll Surg 221:e27–36
45. Nomi T, Hokuto D, Yoshikawa T et al (2018) A novel navigation for laparoscopic anatomic liver resection using indocyanine green fluorescence. Ann Surg Oncol 25:3982
46. Kaibori M, Ishizaki M, Matsui K et al (2011) Intraoperative indocyanine green fluorescent imaging for prevention of bile leakage after hepatic resection. Surgery 150:91–98
47. Takahashi H, Zaidi N, Berber E (2016) An initial report on the intraoperative use of indocyanine green fluorescence imaging in

the surgical management of liver tumors. J Surg Oncol 114:625–629
48. Kaibori M, Matsui K, Ishizaki M et al (2016) Intraoperative detection of superficial liver tumors by fluorescence imaging using indocyanine green and 5-aminolevulinic acid. Anticancer Res 36:1841–1849
49. Miyata Y, Ishizawa T, Kamiya M et al (2017) Intraoperative imaging of hepatic cancers using γ-glutamyltranspeptidase-specific fluorophore enabling real-time identification and estimation of recurrence. Sci Rep 7:3542
50. Daskalaki D, Aguilera F, Patton K et al (2015) Fluorescence in robotic surgery. J Surg Oncol 112:250–256
51. Miyazaki Y, Kurata M, Oshiro Y et al (2018) Indocyanine green fluorescence-navigated laparoscopic metastasectomy for peritoneal metastasis of hepatocellular carcinoma: a case report. Surg Case Rep 4:130